VALIDITY OF DIFFERENT MODELS OF INTERFACES IN ADHESION AND DIFFUSION BONDED JOINTS

Tom Pialucha, Michael Lowe and Peter Cawley
Department of Mechanical Engineering
Imperial College
London SW7 2BX
UK

INTRODUCTION

The need to characterise thin layers between thicker sections of material arises in several current NDE problems, for example the oxide layer between the adhesive and adherend in an adhesively bonded joint, and an interlayer of a different material in a diffusion bonded joint. Many workers have attempted to characterise these layers by ultrasonic reflection coefficient measurements.

In order to predict the reflection coefficient theoretically, the interface layer can be regarded as a discrete layer having its own acoustic properties and thickness. If the interlayer is very small compared with the wavelength of the sound used then thin layer approximations can be employed, the most popular being the spring model first proposed by Tattersall [1] and used by many other groups (see for example refs [2 - 5]). Baik and Thompson [6] have employed a more sophisticated mass-spring model in which the mass of the layer, as well as its stiffness, is taken into account. This paper assesses the range of applicability of the spring and mass-spring models by comparing them with an exact model in which the layer is represented as a continuum.

THIN LAYER APPROXIMATIONS

Consider a flat horizontal isotropic layer of thickness d between two half-spaces as shown in fig. 1. When an infinite plane wave of frequency ω is incident at the bottom face of the layer then the transmitted and reflected waves in the system will form a unique stress and displacement field on both sides of the layer. It is possible to derive an expression relating the stresses and displacements at the top face of the layer as a function of stresses and displacements at the bottom face of the layer. This relationship can be expressed in matrix form as,

$$\mathscr{L} \begin{Bmatrix} \sigma_{22} \\ \sigma_{21} \\ u_1 \\ u_2 \end{Bmatrix}_{\text{bottom}} = \begin{Bmatrix} \sigma_{22} \\ \sigma_{21} \\ u_1 \\ u_2 \end{Bmatrix}_{\text{top}} , \tag{1}$$

where σ_{22}, σ_{21} are the normal and shear stresses, and u_1, u_2 are the horizontal and vertical displacement components in the layer (see fig. 1).

Review of Progress in Quantitative Nondestructive Evaluation, Vol. 12
Edited by D.O. Thompson and D.E. Chimenti, Plenum Press, New York, 1993

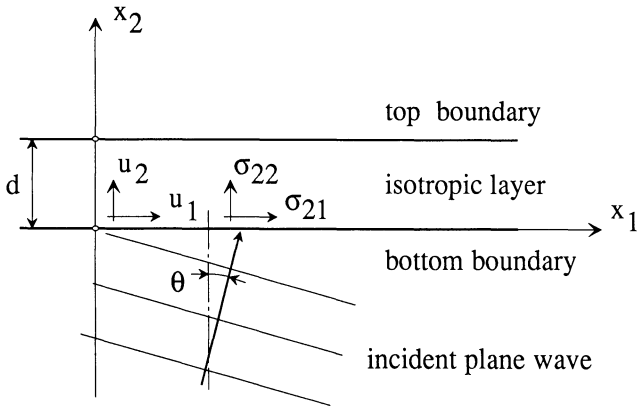

Fig. 1. Coordinate system position with respect to the layer. The infinite plane wave of frequency ω strikes the layer at an angle of incidence θ.

The matrix $\mathscr{L}$ is 4×4 complex and given by,

$\frac{D}{2}G_p + c_S^2 s^2 G_s$	$\frac{c_L s D}{2A}H_p - Bc_S s H_s$	$i\omega\rho D c_S^2 s (G_p - G_s)$	$\frac{i\omega\rho C^2 c_L}{2A}H_p + 2i\omega\rho B c_S^3 s^2 H_s$
$\frac{Ac_S^2 s}{c_L}H_p - \frac{Dc_S s}{2B}H_s$	$c_S^2 s^2 G_p + \frac{D}{2}G_s$	$\frac{2Ai\omega\rho s^2 c_S^4}{c_L}H_p + \frac{i\omega\rho D^2 c_S}{2B}H_s$	$i\omega\rho D c_S^2 s (G_p - G_s)$
$\frac{s}{2i\omega\rho}(G_p - G_s)$	$\frac{c_L s^2}{2Ai\omega\rho}H_p + \frac{B}{2c_S i\omega\rho}H_s$	$c_S^2 s^2 G_p + \frac{D}{2}G_s$	$\frac{c_L s D}{2A}H_p - Bc_S s H_s$
$\frac{A}{2c_L i\omega\rho}H_p + \frac{c_S s^2}{2Bi\omega\rho}H_s$	$\frac{s}{2i\omega\rho}(G_p - G_s)$	$\frac{Ac_S^2 s}{c_L}H_p - \frac{Dc_S s}{2B}H_s$	$\frac{D}{2}G_p + c_S^2 s^2 G_s$

where d is the thickness of the layer, ω is the angular frequency of the incident wave, ρ is the density of the layer, and c_L and c_S are the longitudinal and shear wave velocities in the layer. Parameter s characterises the angle of incidence of the exciting wave and is given by,

$$s = \frac{\sin\theta}{c}, \tag{3}$$

where θ is the angle of incidence and c is the phase velocity of the incident wave. A, B, D, and g_p, g_s are given by,

$$A = (1 - c_L^2 s^2)^{1/2}, \quad B = (1 - c_S^2 s^2)^{1/2}, \quad D = 1 - 2c_S^2 s^2,$$

$$g_p = e^{i\omega A c_L^{-1} d}, \qquad g_s = e^{i\omega B c_S^{-1} d}. \tag{4}$$

The remaining terms G_p, G_s, H_p, H_s are given by,

$$G_p = g_p + g_p^{-1}, \qquad H_p = g_p - g_p^{-1},$$

$$G_s = g_s + g_s^{-1}, \qquad H_s = g_s - g_s^{-1}. \tag{5}$$

The thin layer formulation can be obtained by letting the frequency-thickness product, ωd, of the layer, become small. The values of g_p and g_s of eqn (4) can then be approximated by,

$$g_p \approx 1 + i\omega A c_L^{-1} d, \quad g_s \approx 1 + i\omega B c_S^{-1} d. \tag{6}$$

It follows from eqn (6) that,

$$G_p \approx 2, \qquad H_p \approx 2i\omega A c_L^{-1} d, \qquad G_s \approx 2, \qquad H_s \approx 2i\omega B c_S^{-1} d. \tag{7}$$

The approximation here takes into account only the constant and linear terms of the Taylor expansion with respect to ωd, around $\omega d = 0$. Equations (6) therefore form the basis of the thin layer approximation. Substituting equations (6) and (7) into eqn (1) gives,

$$\begin{bmatrix} 1 & -i\omega sd & 0 & -\omega^2 \rho d \\ i\omega s(2c_S^2 c_L^{-2}-1)d & 1 & -\omega^2\rho[1-4s^2c_S^2(1-c_S^2c_L^{-2})]d & 0 \\ 0 & \frac{1}{\rho c_S^2} d & 1 & -i\omega sd \\ \frac{1}{\rho c_L^2} d & 0 & i\omega s(2c_S^2 c_L^{-2}-1)d & 1 \end{bmatrix} \begin{Bmatrix} \sigma_{22} \\ \sigma_{21} \\ u_1 \\ u_2 \end{Bmatrix}_{\text{bottom}} = \begin{Bmatrix} \sigma_{22} \\ \sigma_{21} \\ u_1 \\ u_2 \end{Bmatrix}_{\text{top}}. \tag{8}$$

Equation (8) is the thin layer approximation of eqn. (1) and is dependent on three parameters: the frequency of excitation ω, the thickness of the layer d, and a variable s, defined in eqn (3) and characterising the angle of incidence of the exciting wave.

When the incident wave propagates in the direction perpendicular to the layer then $\theta = 0$ and, by eqn (3), $s = 0$, so eqn (8) simplifies to,

$$\begin{bmatrix} 1 & 0 & 0 & -\omega^2 m \\ 0 & 1 & -\omega^2 m & 0 \\ 0 & \frac{1}{k_T} & 1 & 0 \\ \frac{1}{k_N} & 0 & 0 & 1 \end{bmatrix} \begin{Bmatrix} \sigma_{22} \\ \sigma_{21} \\ u_1 \\ u_2 \end{Bmatrix}_{\text{bottom}} = \begin{Bmatrix} \sigma_{22} \\ \sigma_{21} \\ u_1 \\ u_2 \end{Bmatrix}_{\text{top}}, \tag{9}$$

where k_N and k_T are respectively the dynamic stiffnesses per unit area of the layer in the directions perpendicular to the plane of the layer (normal stiffness), and parallel to the plane of the layer (tangential stiffness),

$$k_N = \frac{\rho c_L^2}{d}, \qquad k_T = \frac{\rho c_S^2}{d}, \tag{10}$$

and m is the mass of the layer per unit area, given by, $m = \rho\, d$. Equation (9) states that when an isotropic layer is thin and an incident wave (longitudinal or shear) strikes the layer at normal incidence then it is valid to approximate the behaviour of the layer using a simple mass-spring model. In the spring model, the normal and tangential stiffnesses are obtained from eqn (10) and the mass of the layer is neglected.

Comparing eqn (8), derived for a general case of plane wave excitation, with eqn (9) it can readily be seen that a simple mass-spring model simplification may no longer be applicable when an exciting wave strikes the layer at an oblique incidence. It is, however, possible to show that when the shear velocity of the layer is small in comparison to that of the incident wave then eqn (8) simplifies again to the mass-spring model given in eqn (9), even for oblique incidence excitation [7].

LIMITS OF APPLICABILITY OF THE SPRING MODEL

In order to determine the limits of applicability of the spring model let us calculate the normal incidence reflection coefficient from the spring model and compare the results with the normal incidence reflection coefficient from the mass-spring model. For the sake of the argument we will consider longitudinal wave excitation bearing in mind that the same analysis applies to the normal incidence shear wave case (if the system can support shear wave propagation).

Consider a layer of thickness d in between two half spaces as shown in fig. 2, being excited by a longitudinal wave in the direction perpendicular to the layer. Let us denote the half-space extending downwards from the bottom of the layer as medium number 1, the layer as medium number 2, and the top half-space as medium number 3. Each of the three media are given their own densities and wave velocities, ρ_i and c_i, i = 1,2,3. Let us furthermore assume that the layer (medium 2) has been approximated by a mass-spring boundary. The displacement field in the bottom half-space (medium number 1) can be expressed as the sum of two waves: an incident wave of amplitude T_1, and reflected wave of amplitude R_1. In the top half-space, the displacement field will consist of only a single transmitted wave of amplitude T_3.

In general, a longitudinal plane wave propagating in a direction along the x_2 coordinate can be expressed as,

$$u_2(x_2,t) = A\, e^{i\omega(x_2/c-t)} , \tag{11}$$

where u_2 is the displacement field in the x_2 direction, A is the amplitude, ω is the frequency and c is the phase velocity of the wave. The normal stress in the x_2 direction can be calculated from the standard stress-strain equation of the form,

$$\sigma_{22} = E\varepsilon_{22} , \tag{12}$$

where $\varepsilon_{22} = \dfrac{\partial u_2}{\partial x_2}$, and E is an elastic constant, given by $E = \rho c^2$, where ρ is the density of the medium.

Substituting eqn (11) into (12), we have,

$$\sigma_{22}(x_2,t) = i\omega z\, u_2(x_2,t) , \tag{13}$$

where $z = \rho c$, is defined as the impedance of the medium.

Using eqn (9), which was derived for the mass-spring model, the normal stresses and displacements at the top of the layer can be described in terms of the stresses and displacements at the bottom of the layer as,

$$u_2(d) = u_2(0) + \frac{1}{k_2}\, \sigma_{22}(0) , \tag{14}$$

$$\sigma_{22}(d) = \sigma_{22}(0) - \omega^2 m_2\, u_2(0) , \tag{15}$$

where the stiffness of the layer is given by eqn (10), and the mass m_2 of the layer is $\rho_2 d$.

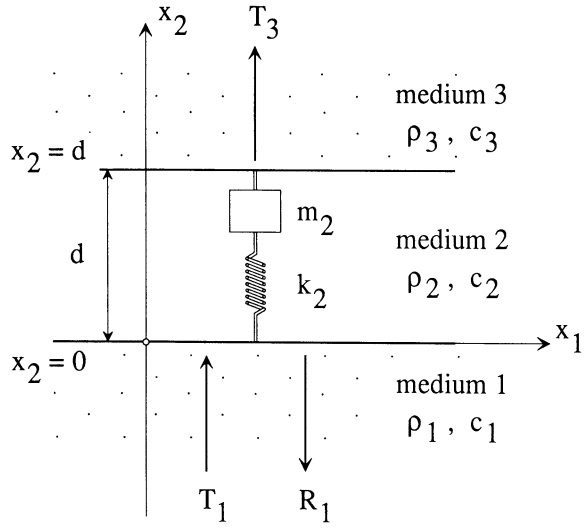

Fig. 2. Mass-spring approximation of a thin layer.

In order to solve the reflection coefficient problem, it is necessary to set the amplitude of the incident wave, T_1, to unity and solve for the amplitude of the reflected wave, R_1. Using equations (11), (14) and (15) the following expression can finally be derived [7],

$$R_1 = \frac{z_1 - z_3 - \frac{i\omega}{k_2}(z_1 z_3 - z_2^2)}{z_1 + z_3 - \frac{i\omega}{k_2}(z_1 z_3 + z_2^2)} . \tag{16}$$

Equation (16) describes the normal incidence reflection coefficient from the mass-spring boundary in terms of its acoustic impedance and stiffness as well as acoustic impedances of the neighbouring half-spaces.

In order to obtain an expression for the reflection coefficient from the spring only boundary, it is necessary to set the mass of the layer to zero. This implies that the impedance of the layer, $z_2 = 0$, so eqn (16) becomes,

$$R_1 = \frac{z_1 - z_3 - \frac{i\omega}{k_2} z_1 z_3}{z_1 + z_3 - \frac{i\omega}{k_2} z_1 z_3} . \tag{17}$$

Having derived the expressions for the reflection coefficients from mass-spring and spring boundaries, it is now possible to find the conditions in which the spring model gives satisfactory approximations. Comparing equations (16) and (17) it can clearly be seen that the spring model will be a satisfactory approximation of the mass-spring model only when the square of the layer's impedance is much smaller then the product of the impedances of the neighbouring half-spaces, that is,

$$z_2^2 << z_1 z_3 . \tag{18}$$

It has been shown in eqn (9) that the mass-spring model approximates the behaviour of thin layers satisfactorily only at low frequency-thickness product, when eqn (6) is satisfied. Therefore, the spring model can be applied successfully only when both equations (6) and (18) are concurrently satisfied.

Table 1 Acoustic properties of materials used in calculations.

material	density ρ (kg/m^3)	longitudinal velocity c_L (m/s)	longitudinal impedance z_L (kg/m^{2}s)
aluminium	2820	6330	17.85 E6
aluminium oxide (70 % porosity)	1170	10400	12.17 E6
epoxy resin	1170	2610	3.05 E6
water	1000	1490	1.49 E6

COMPARISON OF APPROXIMATE MODELS WITH EXACT THEORY

Let us compare the two approximate models to the exact one. The first example is a 0.1 mm thick epoxy layer between two aluminium half-spaces. Material properties of the aluminium and the epoxy are given in Table 1.

Figure 3 shows the normal incidence longitudinal reflection coefficient from the layer. The three different curves on the plot show the predictions of the three different models. As can be seen from the figure, in the low frequency range, the spring model and the mass-spring model approximate the exact solution rather well. This is in accordance with the criterion given by eqn (18), as $z_2^2 = 9.3$ E12 (kg/m^{2}s)^2 and $z_1 z_3 = 319.0$ E12 (kg/m^{2}s)^2, so $z_2^2 << z_1 z_3$. Moreover, since the velocity of the shear wave in epoxy ($c_S = 1170$ m/s) is significanlty smaller than the longitudinal velocity in aluminium ($c_L = 6330$ m/s) then both approximate models can be used to calculate the longitudinal-longitudinal reflection coefficient at oblique incidence. Figure 4 shows the longitudinal-longitudinal reflection coefficient from the layer computed at an angle of incidence of 20 degrees assuming the shear velocity in aluminium, $c_S = 3120$ m/s. Good agreement between the continuous model, the mass-spring model and the spring model can be seen.

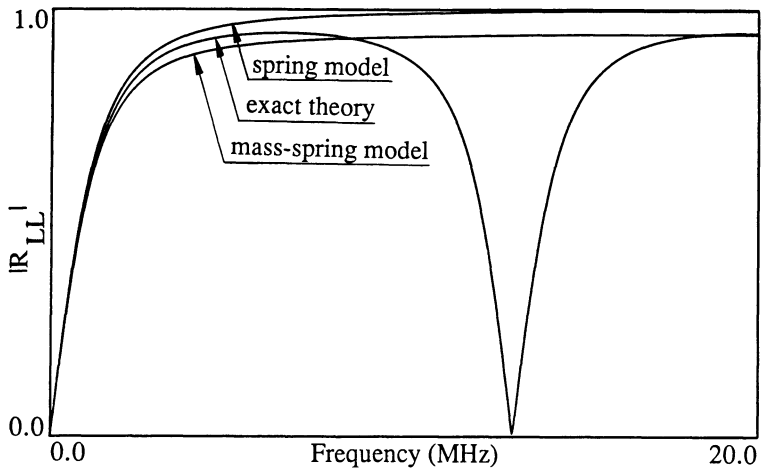

Fig. 3. Amplitudes of the normal incidence longitudinal-longitudinal reflection coefficient from a 0.1 mm thick epoxy layer between aluminium half-spaces. Comparison between the exact solution and the approximate theories.

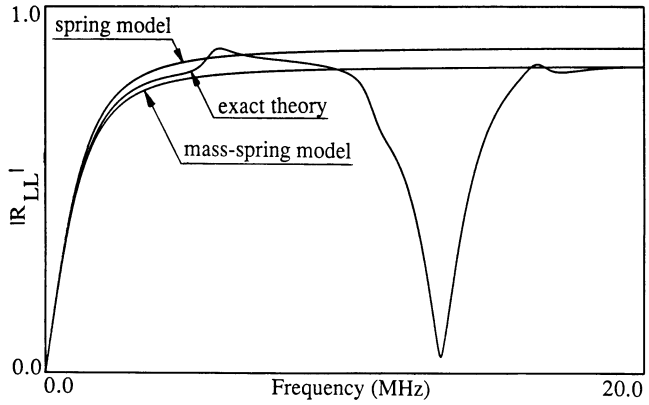

Fig. 4. Amplitudes of the longitudinal-longitudinal reflection coefficient from a 0.1 mm thick epoxy layer between aluminium half-spaces at an angle of incidence of 20 degrees. Comparison between the exact solution and the approximate theories.

Figure 5 shows the normal incidence longitudinal reflection coefficient from a 50.0 μm thick aluminium oxide with assumed porosity of 70%, embedded between aluminium and epoxy half-spaces. Material properties of the aluminium, the oxide and the epoxy are given in Table 1. The mass-spring model approximates the exact theory in the low frequency region rather well. However, the figure shows that the spring approximation generates a reflection coefficient which is an increasing function of frequency, which is the opposite to what the exact theory predicts. Applying criterion given by eqn (18) one can see that z_2^2 = 161.3 E12 $(kg/m^2s)^2$ and $z_1 z_3$ = 54.4 E12 $(kg/m^2s)^2$, and therefore the requirement $z_2^2 << z_1 z_3$ is not satisfied here.

Figure 6 shows the normal incidence reflection coefficient predictions from an oxide wafer in water. As before, material properties of the oxide and water are given in table 1. It can clearly be seen that the spring model fails to model the response of the layer even approximately, while the mass-spring model can be used to accurately predict the behaviour of the layer in the low frequency range. Again, this is in accordance with criterion given by eqn (18), because z_2^2 = 161.3 E12 $(kg/m^2s)^2$ and $z_1 z_3$ = 2.2 E12 $(kg/m^2s)^2$, which means that the relationship $z_2^2 << z_1 z_3$ does not hold here.

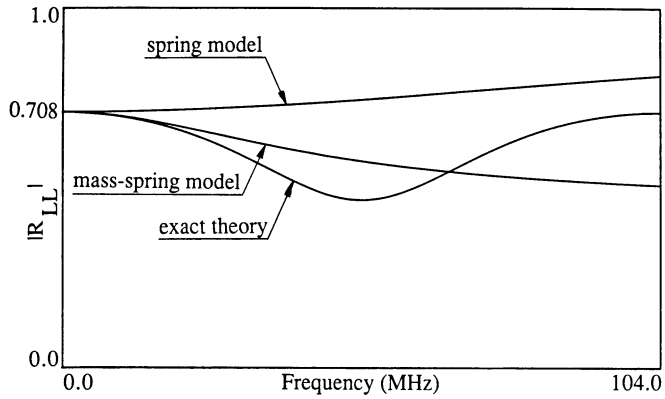

Fig. 5. Amplitudes of the normal incidence longitudinal-longitudinal reflection coefficients from a 50 μm thick oxide layer between aluminium and epoxy half-spaces. Comparison between the exact solution and the approximate theories.

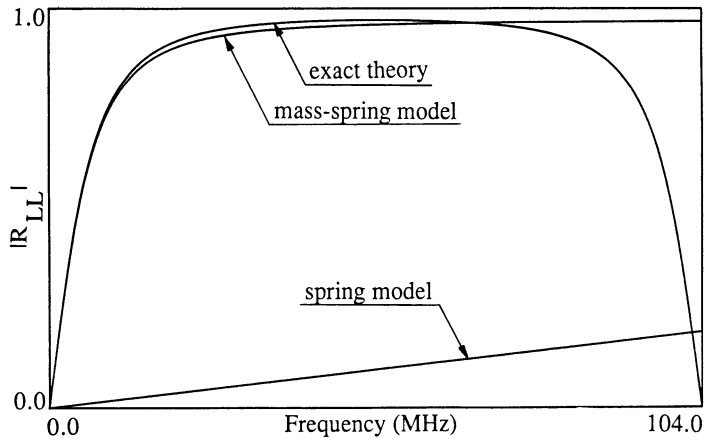

Fig. 6. Amplitudes of the normal incidence longitudinal-longitudinal reflection coefficient from a 50 μm thick oxide layer in water. Comparison between the exact solution and the approximate theories.

CONCLUSIONS

Two different approximate models, the spring model and the mass-spring model, have been compared with the exact isotropic layer model in the case when the thickness of the layer is thin in comparison with the wavelength of the incident wave.

It has been shown that the low frequency-thickness product requirement is not sufficient for the spring or the mass-spring models to be applicable; the neighbouring half-spaces affect the range of applicability of the models.

For normal incidence excitation it has been shown that the spring model can be successfully used as the low frequency approximation when the acoustic impedance of the layer is small in comparison with the impedances of the neighbouring half-spaces. However, when the impedance of the layer is not negligible in comparison with those of the half-spaces then the mass-spring model has to be used as the low frequency approximation of the system.

It has been shown that if the shear velocity of the layer is small in comparison with the speed of the incident wave then the mass-spring approximation can also be used for oblique incidence excitation. Further details of this will be given in [7].

REFERENCES

1. D.E.W. Tattersall, J. Phys. D: Appl. Phys., 6, 819, (1973).
2. N.F. Haines, *The Theory of Sound Transmission and Reflection at Contacting Surfaces*, (Central Electricity Generating Board, RD/B/N4744, 1983).
3. A. Pilarski, Mat. Eval., 43, 765 (1983).
4. A. Pilarski and J.L. Rose, NDT International, 21, 241, (1988).
5. P.B. Nagy, J. Adhesion Sci. Technol, 5,619, (1991)
6. J.M. Baik and R.B. Thompson, J. NDE, 4, 177 (1984).
7. T.P. Pialucha and P. Cawley, 'The reflection coefficient from interface layers - comparisons with thin layer approximations', in preparation.